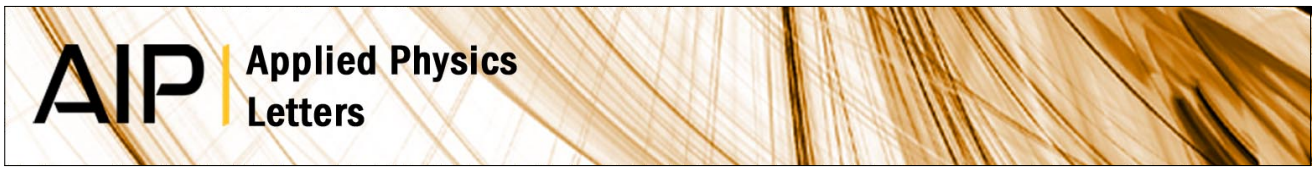

Refractive transmission of light and beam shaping with metallic nano-optic lenses

Zhijun Sun and Hong Koo Kim

Citation: Appl. Phys. Lett. **85**, 642 (2004); doi: 10.1063/1.1776327
View online: http://dx.doi.org/10.1063/1.1776327
View Table of Contents: http://apl.aip.org/resource/1/APPLAB/v85/i4
Published by the AIP Publishing LLC.

Refractive transmission of light and beam shaping with metallic nano-optic lenses

Zhijun Sun and Hong Koo Kim[a)]
Department of Electrical Engineering and Institute of NanoScience and Engineering, University of Pittsburgh, 348 Benedum, Pittsburgh, Pennsylvania 15261

(Received 9 March 2004; accepted 24 May 2004)

We have performed finite-difference time-domain (FDTD) analysis of optical transmission through a nanoslit array structure formed on a metal layer with tapered film thickness. The analysis result shows refractive transmission of light through the nanoslit array, opening up the possibility of creating metallic lenses that resemble glass lenses in their shape. Metallic lenses with curved surfaces are designed such that each nanoslit element transmits light with phase retardation controlled by the metal thickness in the aperture region. The FDTD analysis result demonstrates a focusing or collimating function of convex-shaped metal lenses. © *2004 American Institute of Physics*. [DOI: 10.1063/1.1776327]

Conventional dielectric lenses perform beam shaping via refraction of light at curved surfaces with index contrast. In the language of wave optics, a lens provides proper phase retardation to the optical fields emanating from infinitesimal dipole elements that are continuously distributed on the exit surface of a lens.[1] In diffractive optics, optical fields are changed by means of diffraction through zones of microscale features formed on a dielectric surface.[2] An incident beam diffracts at each zone with different angle, and this has the effect of modulating the phase of the incident field. Whereas dielectric is commonly used in conventional refractive or diffractive optics, utilization of metal in beam shaping has been limited to the nontransmissive mode of operation such as reflection or diffraction.[3] It should, however, be mentioned that nanoapertured metal structures have been drawing increasing attention as an interesting medium for transmissive interactions in the optical frequency range.[4–11] Ebbesen *et al.*, for example, have recently reported experimental observation of an extraordinary transmission of light through subwavelength-hole arrays or through a single hole (or slit) surrounded by surface corrugations.[4,9,10] While this opens up a new avenue for transmissive optics, the potential for metallic refractive optics has not been explored yet.

We report the refractive transmission of light through a metallic nanoslit array and demonstrate beam shaping (focusing or collimating) functions of the convex-shaped metallic lenses. Each nanoslit element in the lens structure is designed to transmit light with a phase relationship controlled by the metal thickness profile of the array lens. The metal-based refractive optics is shown to offer functions that would complement the beam shaping capability of conventional refractive or diffractive optics. Figure 1 shows a finite-difference time-domain (FDTD) simulation of optical transmission (TM polarized and 650 nm wavelength) through an 80-nm-wide single slit formed in a 200-nm-thick silver layer. The dielectric constant $\varepsilon=-16.19+i1.05$ is used for silver.[12] The incident wave excites a surface plasmon (SP) mode at the slit entrance. The SP wave propagates along the slit region with a complex propagation constant, and then decouples into radiation modes at the slit exit, diffracting into all radial directions with a uniform power distribution. In order to establish a quantitative understanding, we analyzed the SP propagation in the slit region by solving the Maxwell's equations with proper boundary conditions, i.e., that the tangential components of the magnetic and electric fields are continuous at the metal/dielectric interface.[13] The surface plasmon wave vector and thus the complex index n_1 are calculated for TM wave propagating in a silver slit region. [See Fig. 2(a).] Here the complex refractive index n_1 relates the surface plasmon wave vector k in the slit region to the wave vector in the air region, $k=n_1k_0$. The real part of the propagation constant is shown to be much larger than the imaginary part, therefore the wave is propagation dominant. For an 80-nm-wide slit formed in silver, for example, n_1 is calculated to be $1.27+i0.01$ at 900 nm wavelength. As the slit width is further reduced, both the real and imaginary parts of index n_1 increase, indicating that the portion of the SP field in the metal region grows.

The transmittance through a slit of finite depth is expressed as follows:

$$A=\left|\frac{\tau_{01}\tau_{12}e^{ikh}}{1+\rho_{01}\rho_{12}e^{i2kh}}\right|, \tag{1}$$

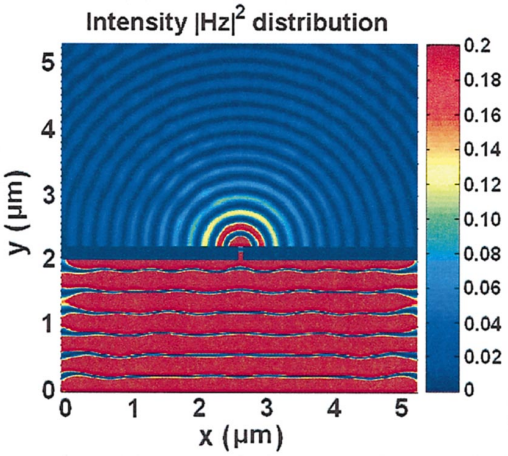

FIG. 1. (Color) Optical transmission through a single nanoaperture (80-nm-wide single slit) formed on a metal layer (200-nm-thick silver): a FDTD analysis of beam propagation. A TM-polarized plane wave (650 nm wavelength) is incident to the slit from the bottom side in the image.

[a)]Electronic mail: kim@engr.pitt.edu

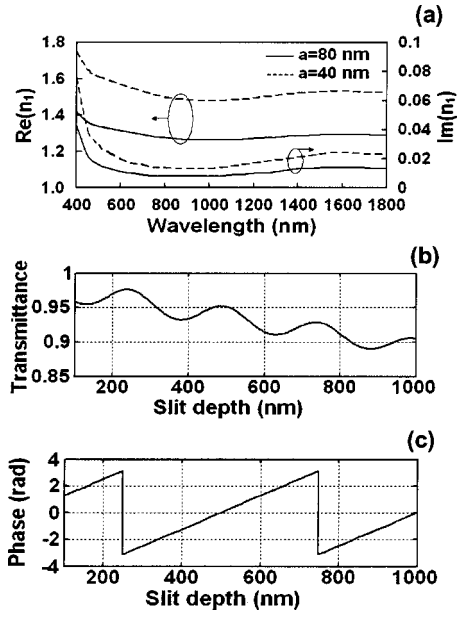

FIG. 2. Characteristics of a surface plasmon wave through a nanoslit structure formed in metal. (a) The complex refractive index, n_1 (the real part in a solid curve and the imaginary part in a dashed curve) calculated for a silver slit (with slit width of 40 or 80 nm). The inside of the slit region is assumed to be air. (b) The transmittance A_a and the phase ϕ_a of the optical field at a nanoslit exit plotted as a function of slit depth h_a. The slit width is assumed to be 80 nm and the wavelength of light is 650 nm. The dielectrics adjacent to the nanoslitted silver layer are assumed to be air.

$$\phi = \phi_{01} + \phi_{12} + n_1 k_0 h - \theta. \tag{2}$$

Subscripts 0, 1, and 2 denote the media before, inside, and after the nanoslit array, respectively, in terms of beam propagation. ρ_{01} and ρ_{12} are the reflectivity of surface plasmon wave at the entrance and exit side of slit/dielectric interfaces, respectively, and are given as $\rho_{01}=(n_0-n_1)/(n_0+n_1)$ and $\rho_{12}=(n_1-n_2)/(n_1+n_2)$. $\phi_{01}=\arg(\rho_{01})$ and $\phi_{12}=\arg(\rho_{12})$. $\tau_{01}=1-\rho_{01}$ and $\tau_{12}=1-\rho_{12}$. n_0 and n_2 are the refractive indices of the media outside the slit array layer. $\theta=\arg(1+\rho_{01}\rho_{12}e^{i2kh})$. h is the slit depth. In general, both the amplitude (i.e., transmittance) A and the phase ϕ are complex functions of the structural and materials parameters (such as slit width, depth and spacing, and dielectric constants) and the operating wavelength relative to slit spacing.[14–19] In the regime where the surface plasmon waves localized at each slit do not couple to a significant degree, both the transmittance (A) and phase (ϕ) of optical field are primarily determined by slit depth, i.e., metal thickness [Figs. 2(b) and 2(c)]. The calculation shows that the amplitude change remains relatively insignificant over a broad thickness range, i.e., with a variation of 0.89–0.98 for the metal thickness of 100–1000 nm in the case of 80 nm slit width. The periodic fluctuation of amplitude indicates the Fabry–Perot resonance of surface plasmon wave in the nanoslit region. The calculation also shows that the phase of optical field is almost linearly proportional to slit depth.

Figure 3 shows FDTD simulation of transmission of light (TM-polarized and 900 nm wavelength) through a three-slit structure. 80-nm-wide slits are introduced on a Ag layer with 370 nm slit spacing, and the Ag layer thickness is varied with a 50 nm step profile such that the slit depth becomes 250, 300, and 350 nm in sequence. The different slit depth is to introduce phase retardation among the radiation

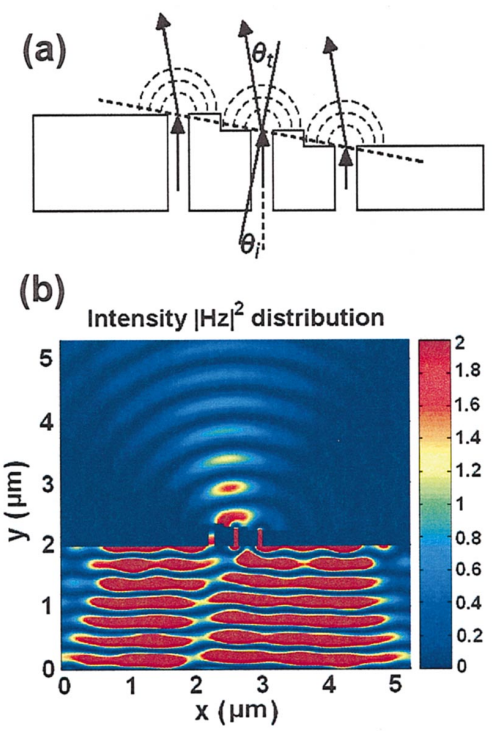

FIG. 3. (Color) Refractive transmission of light through a nanoslit array formed in a metal layer with tapered metal thickness. (a) A schematic drawing of a three-slit structure with tapered metal thickness. 80-nm-wide slits are introduced on a Ag layer with a 370 nm spacing, and the metal thickness is varied with a 50 nm step profile such that the slit depth becomes 250, 300, and 350 nm in sequence. (b) A FDTD simulation of optical transmission through the slit array. A TM-polarized plane wave (900 nm wavelength) is incident to the bottom side of the slit array.

components at the exit surface of metal. The FDTD analysis result clearly reveals that the transmitted beam propagates along the direction tilted toward the thicker side of metal. This behavior is reminiscent of the refraction of light in conventional dielectric optics. This observation is corroborated with the following simple analysis. The optical fields (the magnetic field H_z) in the far-field regime of a beam transmitted through a nanoslit array can be expressed as a summation of the cylindrical waves from each nanoslit element,

$$H_z(x,y) = \sum_{\alpha} \frac{A_\alpha}{\sqrt{r_\alpha}} e^{i\phi_\alpha} e^{ik_o r_\alpha}. \tag{3}$$

Here, $r_\alpha=\sqrt{(x-x_\alpha)^2+(y-y_\alpha)^2}$, and k_0 is the wave vector of the transmitted beam in the air region. A_a and ϕ_a are, respectively, the amplitude and phase of the radiation component emanating from the αth slit located at (x_a, y_a), and can be expressed as Eqs. (1) and (2) if we assume no resonance coupling occurs between the neighboring slits. It can be shown that the transmitted waves through the nanoslit array will beam into the direction that satisfies the following phase matching condition at the metal/air interface: $k_{sp} \sin \theta_i = k_0 \sin \theta_t$. Here θ_i is the incidence angle of the surface plasmon wave to the hypothetical planar surface that comprises the slit apertures, and θ_i is the tilt angle of the transmitted beam. This formula basically tells that light will refract at the nanoapertured metal surface in a way similar to that at a dielectric interface. From the phase matching condition and the information on the nano-optic structure shown in Fig. 3 (the index ratio of 1.27 and the incident angle θ_i of 9°), the transmission angle θ_t is calculated to be 11°, which shows a

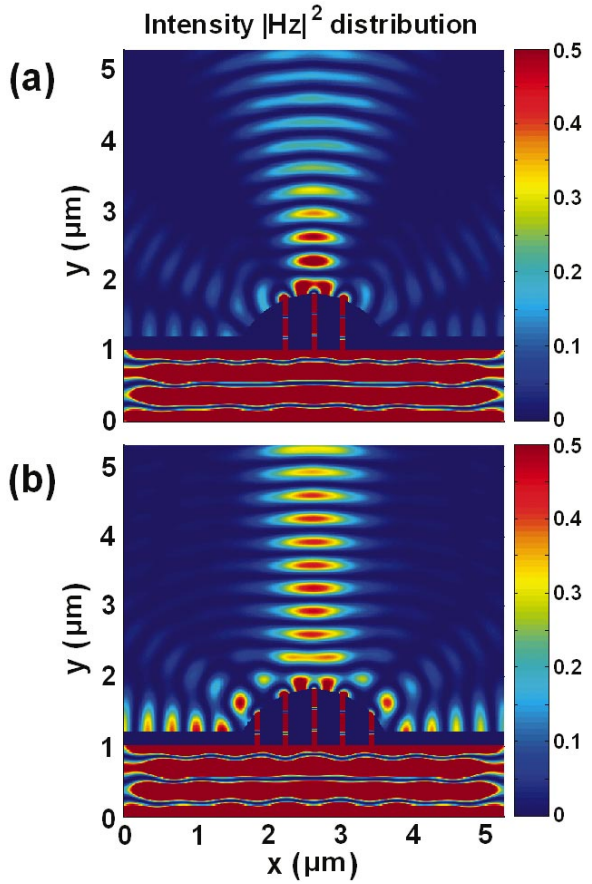

FIG. 4. (Color) FDTD simulations of beam shaping with metallic nanoslit array lenses. The 2-μm-wide convex region is designed to accommodate up to five slits (80-nm slit width) with 400-nm slit spacing, and slit depth of 450, 700, 750, 700, and 450 nm. Beam shaping with (a) a three-slit lens and (b) a five-slit lens structure. A TM-polarized light (650 nm wavelength) is incidnet from the bottom side.

reasonable match to the angle observed in the FDTD simulation ($\sim 13°$). It should be noted that the slit spacing in this design is smaller than the wavelength of light. Therefore, no grating diffraction effect is involved in the optical transmission through the nano-optic structure, unlike the diffractive optics case. The FDTD simulation result demonstrates that the nanoslit arrays with tapered metal thickness possess the capability of beam shaping in a way that resembles the dielectric-based refractive optics (i.e., refraction through curved surfaces) but that is distinctly different from the conventional optics in its mechanism. Figure 4 shows FDTD simulations of beam shaping with nanoslit array lenses that have convex profiles in their metal thickness. The convex region is 2-μm wide and accommodates up to five slits (80-nm slit width) with 400-nm slit spacing (center to center). The metal thickness is designed to vary in a half-elliptical profile such that the slit depth in the array is 450, 700, 750, 700, and 450 nm. Figure 4(a) shows the beam shaping (TM-polarized and 650 nm wavelength) with a three-slit lens structure. The incident beam becomes sharply focused right after the lens with a beam waist of ~ 500 nm. In the case of a five-slit lens structure [Fig. 4(b)], the incident beam becomes focused after the lens and remains well collimated with negligible divergence even after many wavelengths of propagation in the far field region. This indicates an increase of focal length in the five-slit lens compared to the three-slit case. While the shape(geometry)-controlled beam-shaping of metallic lenses resembles conventional refractive optics, the mechanisms involved in optical interactions are distinctly different, and as such their beam-shaping characteristics. The discrete distribution of propagation channels (nanoslit arrays) across a metallic lens is contrasted to the continuous nature of a conventional refractive lens, analogous to digital versus analog. The discrete nature of apertures that emit radiation with proper phase relationship also resembles the phased-array antennas used in the microwave regime.[20]

In conventional dielectric lenses, a transmitted beam shows a strong diffraction effect at lens edges, and this becomes one of the limiting factors in scaling down conventional optics components to a wavelength or subwavelength range. In contrast, the nanoaperture array lenses do not suffer from the edge effect. It is worth mentioning that the phase of each nanoslit element can also be controlled by adjusting other structural and/or materials parameters of nanoslits (such as slit width or the dielectric constant in the slit region) besides slit depth. All these features of metal refractive optics are useful for individual and independent control of phase at each slit, and offer great flexibility in designing the nano-optic lenses that can shape arbitrary beam profiles without being restricted by the constraints of conventional optics.

[1]M. Born and E. Wolf, *Principles of Optics*, 7th ed. (Cambridge University Press, New York, 1999).
[2]*Diffractive Optics and Optical Microsystems*, edited by S. Martellucci and A. N. Chester (Plenum, New York, 1997).
[3]H. Raether, *Surface Plasmons*, edited by G. Hohler (Springer, Berlin, 1988).
[4]T. W. Ebbesen, H. J. Lezec, H. F. Ghaemi, T. Thio, and P. A. Wolff, Nature (London) **391**, 667 (1998).
[5]H. F. Ghaemi, T. Thio, D. E. Grupp, T. W. Ebbesen, and H. J. Lezec, Phys. Rev. B **58**, 6779 (1998).
[6]A. Degiron, H. J. Lezec, W. L. Barnes, and T. W. Ebbesen, Appl. Phys. Lett. **81**, 4327 (2002).
[7]L. Martín-Moreno, F. J. Garcia-Vidal, H. J. Lezec, K. M. Pellerin, T. Thio, J. B. Pendry, and T. W. Ebbesen, Phys. Rev. Lett. **86**, 1114 (2001).
[8]E. Altewischer, M. P. van Exter, and J. P. Woerdman, Nature (London) **418**, 304 (2002).
[9]T. Thio, K. M. Pellerin, R. A. Linke, H. J. Lezec, and T. W. Ebbesen, Opt. Lett. **26**, 1972 (2001).
[10]H. J. Lezec, Science **297**, 820 (2002).
[11]W. L. Barnes, A. Dereux, and T. W. Ebbesen, Nature (London) **424**, 824 (2003).
[12]*Handbook of Optical Constants of Solids*, edited by E. D. Palik (Academic, New York, 1998).
[13]Propagating modes in a metal-clad-dielectric-slab waveguide structure had previously been analyzed for the case that the penetration depth into metal clads is negligible compared to the dielectric slab thickness. See, for example, T. Takano and J. Hamasaki, IEEE J. Quantum Electron. **QE-8**, 206 (1972). In the present work, we analyzed the nanoslit structure by taking into account the effect of field penetration into the metal region without any approximation.
[14]U. Schroeter and H. Heitmann, Phys. Rev. B **58**, 15419 (1998).
[15]J. A. Porto, F. J. García-Vidal, and J. B. Pendry, Phys. Rev. Lett. **83**, 2845 (1999).
[16]S. Astilean, Ph. Lalanne, and M. Palamaru, Opt. Commun. **175**, 265 (2000).
[17]Q. Cao and P. Lalanne, Phys. Rev. Lett. **88**, 057403 (2002).
[18]F. J. García-Vidal, H. J. Lezec, T. W. Ebbesen, and L. Martín-Moreno, Phys. Rev. Lett. **90**, 213901 (2003).
[19]Z. Sun, Y. S. Jung, and H. K. Kim, Appl. Phys. Lett. **83**, 3021 (2003).
[20]J. D. Kraus, *Electromagnetics*, 4th ed. (McGraw–Hill, New York, 1992)